

# High ionic conductive PVDF-based fibrous electrolytes

Zhiming Li · Feng Shan · Jiangong Wei · Jun Yang ·  
Xinsong Li · Xinling Wang

Received: 12 January 2008 / Accepted: 28 February 2008 / Published online: 28 March 2008  
© Springer-Verlag 2008

**Abstract** The high ionic conductive polymer electrolytes were prepared based on poly(vinylidene fluoride) (PVDF) fibers modified via preirradiation grafting poly(methyl methacrylate) (PMMA). In these polymer electrolytes, the PVDF fibers served as the supporting phase providing dimensional stability, and PMMA acted as the gel phase helping for the trapping liquid electrolyte and substituting the nonconductive PVDF phase to provide contact with electrodes well thus increasing conductive area. The modified PVDF fibrous membranes were used as a polymer electrolyte in lithium ion battery after they were activated by uptaking 1 M  $\text{LiPF}_6$ /ethylene carbonate–dimethyl carbonate (1:1 vol) liquid electrolyte, which showed a much higher room-temperature ionic conductivity than the pristine PVDF fibrous membrane. The  $\text{LiCoO}_2$ -mesocarbon microbead coin cells containing the dual-phase fibrous membrane (degree of graft, 111.8%) demonstrated excellent rate performance, and the cell still retained about 86% of discharge capacity at 4C rate, as compared to that at 0.1C rate. The prototype cell showed good cycle performance.

**Keywords** PVDF fibrous membrane · PMMA ·  
Preirradiation · Polymer electrolytes

## Introduction

In the recent few years, lithium ion battery using polymer electrolytes has been known as a preferred power source for various applications because of its high energy density, long life cycle, and memory-free effect [1, 2]. The development of polymer electrolytes having high room-temperature ionic conductivity, less electrolyte leakage, high dimension stability, and good electrochemical stability represents a crucial step in the evolution of polymer electrolyte for lithium ion battery [3–7].

The electrospinning mat is a fibrous membrane composing of ultrafine fibers with a diameter from several tens of nanometers to micrometers. This fibrous membrane can hold a large quantity of liquid electrolyte, since it contains more fully interconnected open cavities, with porosity from 30% to 90%. It is possible for this fibrous membrane applied in thinner battery packs to show high ionic conductivity and greatly to increase battery energy density per weight as compared with conventional polymer battery [8].

A few reports have studied fibrous membranes for polymer electrolytes. Cho et al. investigated poly(acrylonitrile) (PAN) fiber-based polymer electrolytes [9]. The electrochemical properties of PAN fiber-based polymer electrolytes were significantly enhanced by the swelling of the electrospinning PAN fibers. However, the PAN fiber-based framework was observed to swell in an electrolyte solution, which damaged the dimensional stability of the polymer electrolytes. In addition, PAN-based electrolytes underwent severe passivation upon contact with a lithium metal anode [10]. On account of excellent mechanical properties and electrochemical stability, highly crystalline poly(vinylidene fluoride) (PVDF) nanofibrous membrane and its battery application had been studied by Choi et al. [11]. The polymer electrolytes had sufficient mechanical strength because of the remaining crystalline phase in the fibrous membrane. However, its poor affinity ability of its liquid

Z. Li · F. Shan · J. Wei · J. Yang · X. Wang (✉)  
School of Chemistry and Chemical Technology,  
Shanghai Jiao Tong University,  
800 Dongchuan Road,  
Shanghai 200240, People's Republic of China  
e-mail: xlwang@sjtu.edu.cn

X. Li  
School of Chemistry and Chemical Engineering,  
Southeast University,  
Nanjing 211189, People's Republic of China

electrolyte and large open cavities in its fibrous membrane might result in liquid leakage. The Poly(vinylidene fluoride-co-hexafluoropropylene) (P(VDF-HFP)) copolymer was easily wetted by the electrolyte solution. The P(VDF-HFP) fibrous membrane possessed a high uptake and low leakage of the electrolyte solution [12]. Nevertheless, the P(VDF-HFP) copolymer showed less thermal stability than the high-crystalline PVDF. A perfect solution for polymer electrolytes was not easily achieved by conventional fibrous membranes. A mixture of PVDF and poly(methyl methacrylate) (PMMA) might be a good method to achieve high-performance polymer electrolytes [13, 14]. However, the high crystallinity of PVDF limited interdiffusion between PVDF and PMMA. In addition, PMMA could be dissolved in liquid electrolyte, which would result in the macrophase separation between PMMA and PVDF.

To overcome the dilemma, we have prepared the fibrous membrane consisting of dual phases. One phase served as the mechanical supporter (supporting phase), and the other helped for trapping the liquid electrolyte (gel phase). The target was that polymer electrolytes showed higher ionic conductivity and better dimensional stability.

In this work, the PVDF fibrous matrix was chosen as the supporting phase due to good mechanical properties and electrochemical stability and PMMA as the gel phase because of its good affinity for liquid electrolytes and compatibility with electrodes of the lithium ion battery [15, 16]. Radiation-induced grafting copolymerization was an effective method to modify the polymer [17]. Simultaneous radiation grafting (the mixture of the polymer matrix and monomer are irradiated) and preirradiation grafting (the polymer matrix was activated in a preirradiation step and then grafted with the monomer in a subsequent step) were two common methods for radiation grafting [18]. In the preirradiation grafting polymerization, the grafting reaction was easily controlled, and less homopolymer was produced [19]. The dual-phase fibrous membrane was prepared via the preirradiation graft method. The preparation and characterization of the dual-phase fibrous membrane were investigated. The electrochemical properties of this membrane were also studied. Primary results showed that it was a large potential polymer electrolyte for a scaled-up lithium ion battery.

## Experimental

### Materials and preparation of PVDF/PMMA membranes

PVDF fibrous membrane was kindly provided by Professor Xinsong Li from Southeast University. Methyl methacrylate (MMA) was distilled under reduced pressure and stored in a refrigerator. The other reagents and solvents were local commercial products and used without further purification.

The PMMA/PVDF dual-phase fibrous membrane was prepared via the preirradiation grafting method. It was accomplished by first irradiating the PVDF fibrous membrane at room temperature under an air atmosphere using a 2.5-MeV Van de Graaf accelerator. The membrane was irradiated at an absorbed dose  $D$  of 50–150 kGy (dose rate=500 kGy/h) and stored in a refrigerator. Before grafting, the irradiated membrane was cut ( $\sim 2 \times 4 \text{ cm}^2$ ) and immersed at room temperature into a grafting tube containing MMA and ethanol. Then, nitrogen was bubbled in for 15 min in a grafting tube to remove oxygen. The tube was hermetically closed and put into a water bath at 60 °C. After grafting, the membrane was extracted in a Soxhlet extractor with trichloromethane to remove the homopolymer. Then, it was dried to constant mass, and the degree of graft (DOG) was determined gravimetrically; DOG was defined as follows:

$$\text{DOG} = [(m_g - m_o) / m_o] \times 100\% \quad (1)$$

where  $m_g$  and  $m_o$  refer to the mass of the initial and grafted membranes, respectively.

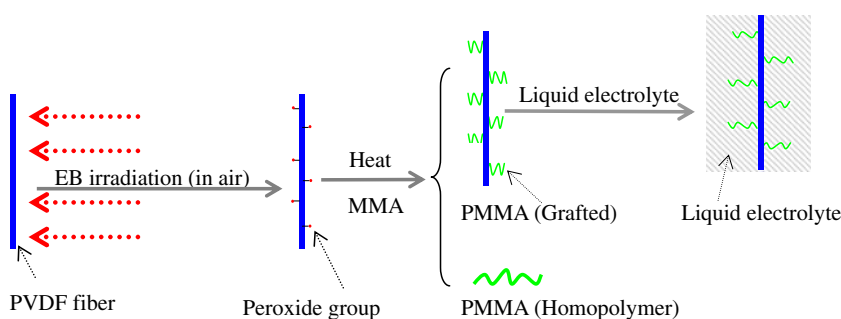
### Characterization and instruments

Attenuated total reflectance Fourier transform infrared spectroscopy (FTIR-ATR) spectra of the surface-grafted membranes were obtained from a Perkin-Elmer Paragon 1000 spectrometer using a ZnSe prism with an incident angle of 45°. Each spectrum was collected by cumulating 64 scans at a resolution of 2  $\text{cm}^{-1}$ . A Field emission scanning electron microscope (FESEM) image of the membrane surface was observed on JEOL JSM 7401F with gold-sputtered coated films at an activation voltage of 5 kV. Thermal gravimetric analysis (TGA) was used to investigate the thermal stability of membranes from a Perkin-Elmer thermal gravimetric analyzer (TGA-7). The samples (about 10 mg) were heated from ambient temperature to 800 °C in a nitrogen atmosphere, and the heating rate of 10 °C/min was used in all cases. The measurements of liquid electrolyte uptake and liquid electrolyte leakage were in accordance with others [12]. The polymer electrolyte membrane was sandwiched between two stainless steel blocking electrodes. The ionic conductivities of the polymer electrolytes were obtained from the bulk resistance ( $R_b$ ) measured by alternating current (AC) impedance analysis using a Solatron 1287 frequency response analyzer over a frequency range of 10 Hz–100 kHz at an amplitude of 5 mV. The ionic conductivity ( $\sigma$ ) of the polymer electrolyte was determined as follows:

$$\sigma = t / (R_b A) \quad (2)$$

where  $t$  is a thickness of the membrane and  $A$  is a surface area of the membrane.

**Fig. 1** Schematic representation of the process of grafting PMMA onto the PVDF fiber via preirradiation and the gelatinization behavior of the PMMA layer in the liquid electrolyte



Assembling and testing of model cells were as follows. The anode was prepared by coating the slurry of meso-carbon microbeads (MCMB; 90%), PVDF binder (7%), and acetylene black (3%) onto a copper foil with a doctor blade. The cathode slurry containing the same PVDF binder (6%) and acetylene black (4%) along with  $\text{LiCoO}_2$  (90%) cathode material was cast on an aluminum foil. The thickness of the electrodes ranged from 60 to 80  $\mu\text{m}$ . The coated electrodes were dried under vacuum at 120  $^\circ\text{C}$  for 8 h. The coin cells were assembled by sandwiching fibrous membrane between the anode and cathode in an argon-filled glove box. Charge–discharge performance of the coin cells was characterized on a battery-testing system (RF-T, Roofer Group, China) between 2.5 and 4.2 V. In the rate property test, the cell was charged at  $C/10$  rate to 4.2 V and then discharged at different current densities to 2.5 V. In the cycle test, the cell was measured in the following order: preconditioning with cutoff voltages of 4.2 V for the upper limit and 2.5 V for the lower limit at the  $C/10$  rate for the first preconditioning cycle and subsequent cycling at  $0.5C$  rate.

**Results and discussion**

**Preparation of the dual-phase fibrous membrane**

The dual-phase fibrous membrane was prepared by grafting PMMA onto a PVDF fiber (PVDF-g-PMMA) via preirradiation grafting. Before grafting reaction, the PVDF fibrous membranes were irradiated in air by an electron beam. When the irradiated membranes were in contact with air, peroxy radicals ( $\text{POO}\cdot$ ) were produced from alkyl radicals ( $\text{P}\cdot$ ) reacting with oxygen.  $\text{POO}\cdot$  recombined to form alkylperoxides (POOP) and/or alkylhydroperoxides (POOH). Grafting reaction on peroxidized polymers usually proceeds via thermal decomposition of peroxides and hydroperoxides to produce the alkoxy radicals ( $\text{PO}\cdot$ ), which initiate radical polymerization of monomers. The process of grafting PMMA onto the PVDF fibrous membrane was illustrated in Fig. 1.

Figure 2 showed the variation of the DOG with reaction time and the irradiation dose. The reaction rate reached the maximum after reacting for about 40 min; the maximum DOG (saturation DOG) was obtained after reacting for

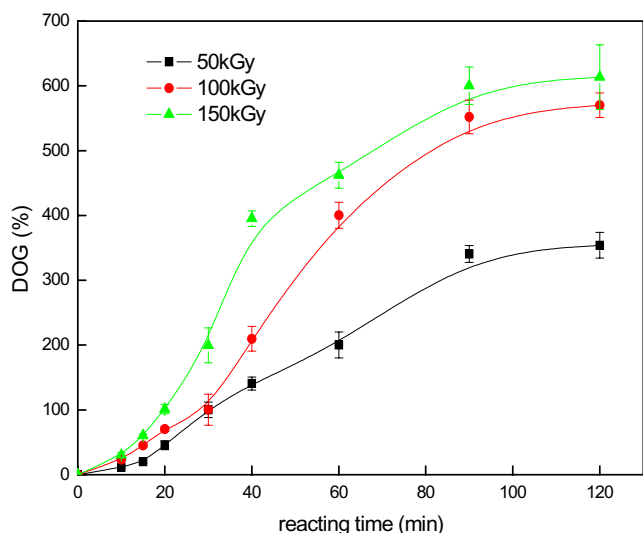


**Fig. 2** Variation of the DOG with reaction time. Monomer concentration, 10%; reaction temperature, 60  $^\circ\text{C}$

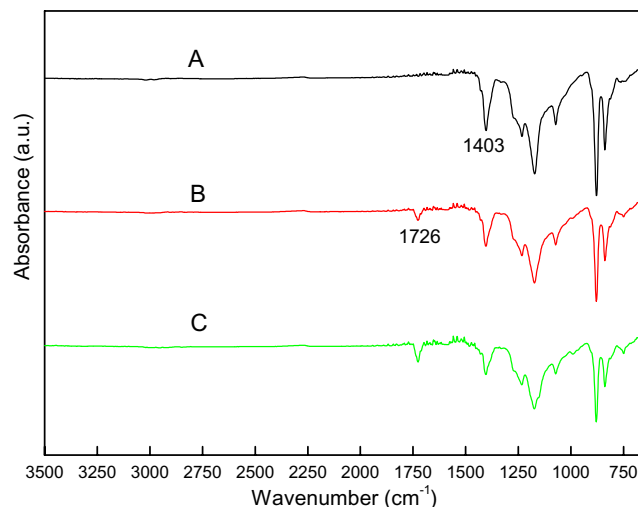
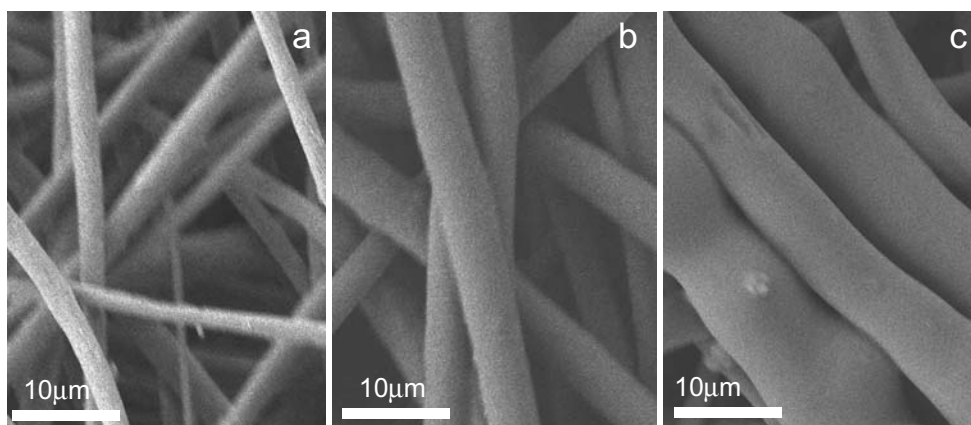


**Fig. 3** FTIR-ATR spectra of pristine PVDF and PVDF-g-PMMA samples: A pristine PVDF, B DOG=40.5%, C DOG=71.2%

**Fig. 4** FESEM images of the nonwoven PVDF membrane grafted by PMMA. **a** DOG=0%; **b** DOG=111.8%; **c** DOG=315.1%



90 min. Both the reaction rate and the saturation DOG were increased with the increase in irradiation dose. It was in agreement with the results from other polymeric systems. Mohr's salt was often used as an inhibitor of the homopolymer in the irradiation graft system. However, there was no obvious inhibition effect in this system. It was possible that the reaction time was relatively short and the monomer concentration was low. On the other hand, ethanol (as the solvent in the grafting reaction system) might reduce the generation of the PMMA homopolymer at a certain degree.

The thicknesses of the fibrous membrane changed with different DOGs. When the DOG was 40.5%, the membrane thickness slightly increased from 75 (pristine membrane) to 78  $\mu\text{m}$ ; when the DOG was increased to 111.8%, its thickness was increased to 84  $\mu\text{m}$ . The results showed that the thickness increase in the grafted fibrous membrane was quite different from the compact membrane (without cavities in membrane). The reason might be that there were a lot of cavities in the fibrous membrane (as shown in Fig. 4), which could provide much room for the PMMA-grafted layer, so the apparent thickness increase was not very obvious. However, the thickness in the compact membrane would be expected to increase rapidly with the increase in DOG because no room could be provided in the membrane.

#### Evidences of dual-phase fibrous membranes

The grafted PMMA was ascertained by FTIR-ATR spectra. The stretching of the PMMA C=O was at  $1,726\text{ cm}^{-1}$ , and the bending of PVDF C-F is at  $1,403\text{ cm}^{-1}$ . In Fig. 3a, no absorption peak of  $1,726\text{ cm}^{-1}$  was observed, but in Fig. 3b and c, the absorption peak of C=O ( $1,726\text{ cm}^{-1}$ ) was found after PMMA was grafted onto PVDF. With the increase in DOG, the intensity of the absorption bands of C=O increased, but that of C-F decreased. These results confirmed that PMMA was successfully grafted onto PVDF.

The effect of grafting upon the surface morphology of the fibrous membrane was investigated by FESEM micro-

graphs. The micrographs of the pristine PVDF fibers and PVDF fibers grafted with PMMA were shown in Fig. 4. It was clear that the grafting of PMMA onto PVDF fibers made the fibers fatter.

The TGA graph of the original PVDF and PVDF-*g*-PMMA at different DOGs was shown in Fig. 5. It was seen that pristine PVDF underwent a single-step degradation, which started at  $430\text{ }^\circ\text{C}$ . The grafted membranes showed a two-step degradation pattern. The first degradation step at  $330\text{ }^\circ\text{C}$  was related to the decomposition of the grafted PMMA. The second loss at  $430\text{ }^\circ\text{C}$  was due to the decomposition of PVDF. In PVDF-*g*-PMMA, two typical degradation temperatures and weight losses for PVDF and PMMA showed the formation of the phase separation structure because of the incompatibility between PVDF and PMMA.

#### Liquid electrolyte uptake and leakage properties

Figure 6 showed the uptake of liquid electrolyte (1 M  $\text{LiPF}_6$ /ethylene carbonate–dimethyl carbonate [EC-DMC])

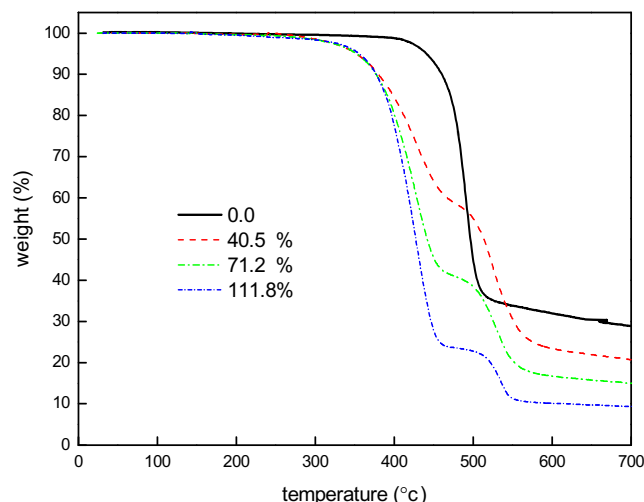


**Fig. 5** TGA thermograms of PVDF with different PMMA content. Heating rate  $10\text{ }^\circ\text{C}/\text{min}$

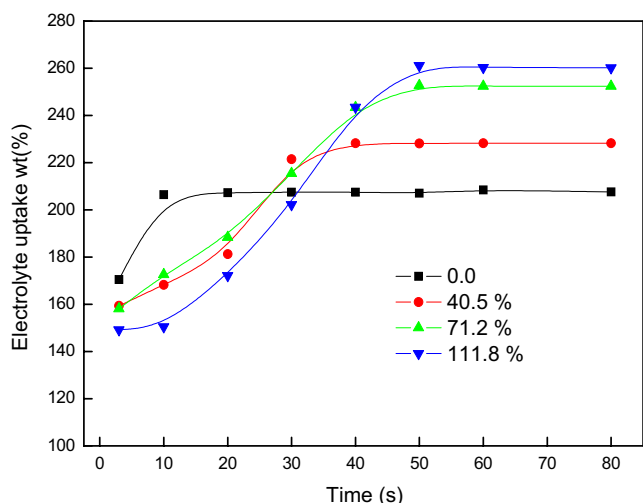


**Fig. 6** The liquid electrolyte uptake of PVDF fibrous membranes with different PMMA contents as the function of soaking time, 25 °C

for pristine and different DOG PVDF fibrous membranes as the function of soak time. In the pristine PVDF fibrous membrane, the liquid electrolyte uptake process was very fast, and the maximum amount of electrolyte that penetrated into the membrane was within a few seconds. The fully interconnected cavity structure in the membrane was beneficial in achieving this. Grafted PVDF fibrous membranes needed more time to reach a saturated state since the PMMA-grafted layer absorbed liquid electrolyte via gelatinization. On the other hand, different DOGs had an influence on the liquid electrolyte absorptive capability. As showed in Fig. 6, the increase in the DOG from 0% to 111.8% led to the increase in electrolyte uptake of fibrous membranes from 210% to 260%. This was due to the good affinity of PMMA for the liquid electrolyte. In this study, the

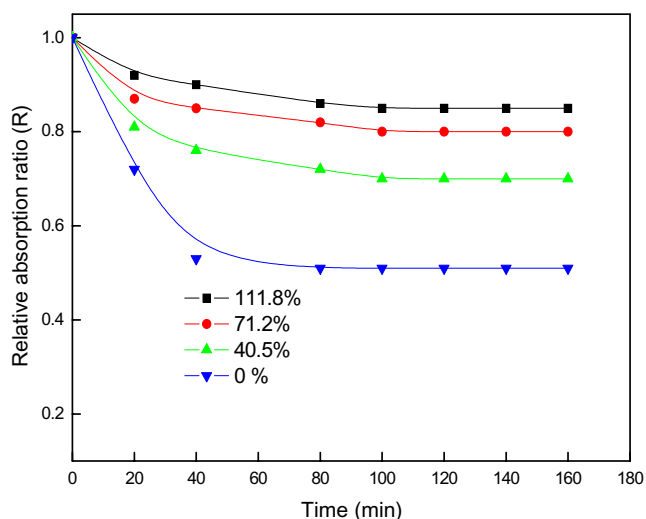


**Fig. 7** The liquid electrolyte leakage of PVDF fibrous membranes with different PMMA contents as the function of leaking time, 25 °C

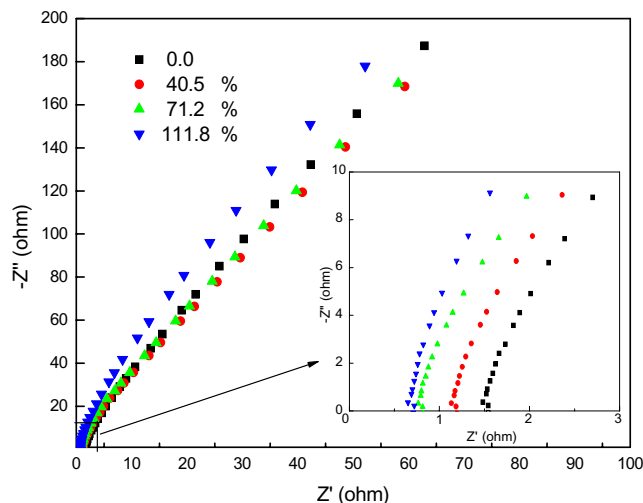


**Fig. 8** AC impedance plots of the nonwoven PVDF membrane with different PMMA contents, 25 °C

absorptive capacity of grafted fibrous membranes became greater with the increasing in DOG, but excessively high DOG would embrittle the fibrous membrane due to the high  $T_g$  of PMMA. Figure 7 showed the liquid leakage of pristine and different DOG PVDF fibrous membranes. The loss of liquid electrolyte in pristine membrane was about 50%. This was because the cavities in pristine PVDF fibrous membrane were quite large (~10 μm) and interconnected, and because of this, liquid leakage took place more easily. The grafted layer (PMMA), which had good affinity for the electrolyte, could preserve more of the electrolyte from leakage. Additionally, after the grafted membranes were soaked in the liquid electrolyte, the outstretched PMMA chains would make the fibers expand, as illustrated in Fig. 1, which led to the decrease in size of cavities in the grafted fibrous membrane. Therefore, the introduction of PMMA onto the PVDF fiber was an effective way to enhance electrolyte uptake and decrease liquid leakage.

**Electrochemical properties**

The fibrous membranes were activated by the 1-M LiPF<sub>6</sub>/EC-DMC (1:1 vol) electrolyte solution. Figure 8 showed typical AC impedance spectra of the activated membranes at room temperature (25 °C). Under the ideal condition, the AC impedance spectroscopy could be represented as Fig. 9.

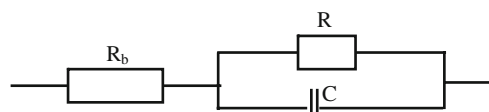


**Fig. 9** Equivalent circuit of AC impedance

$R_b$ ,  $C$ , and  $R$  represented for the bulk resistance of the polymer electrolyte, interfacial capacitance, and the kinetics of the electrochemical reaction between the electrode and sample interfaces, respectively. Behavior of the parallel combination of  $R$  and  $C$  was represented by a characteristic semicircle dispersion of the real ( $Z'$ ) and imaginary ( $-Z''$ ) components of the impedance spectrum. However, a high-frequency semicircle expected for parallel  $R$  and  $C$  was not obtained; it was thought that the  $R$  of the polymer electrolyte was low, and the maximum frequency was limited to 100 kHz. A similar result was obtained by other investigation [20]. It was observed in Fig. 8 that the AC impedance value was very low. The high porosity, the interconnected cavities, and high liquid uptake of polymer electrolyte membranes were beneficial for ions to migrate, which resulted in low impedance. The room-temperature ionic conductivity of pristine the PVDF fibrous membrane was  $2.3 \times 10^{-3} \text{ S cm}^{-1}$ . The ionic conductivity was increased with the increase in DOG. When the DOG was 111.8% (the sample was studied in the following), the ionic conductivity was increased to  $7.9 \times 10^{-3} \text{ S cm}^{-1}$ , which was close to that of liquid electrolyte. It was because grafted membranes had a higher liquid electrolyte uptake. On the other hand, the gelled PMMA layer (ion conductor) replaced PVDF fibers (ion insulator) to be in contact with electrodes, which resulted in an increase in conducting area.

Figure 10 illustrated the temperature dependence of the conductivity for the fibrous membrane. From the figure, it was evident that the plot of  $\log \sigma$  vs.  $1/T$  was a curved line rather than a linear one. It was fitted to the equation of  $Y = -7.56 + 3.67X - 0.617X^2$ , and the error of the regression parameter ( $R^2$ ) was 0.999. Therefore, it was generally observed for highly viscous electrolytes or amorphous polymeric systems [21]. Thus, the ionic conduction

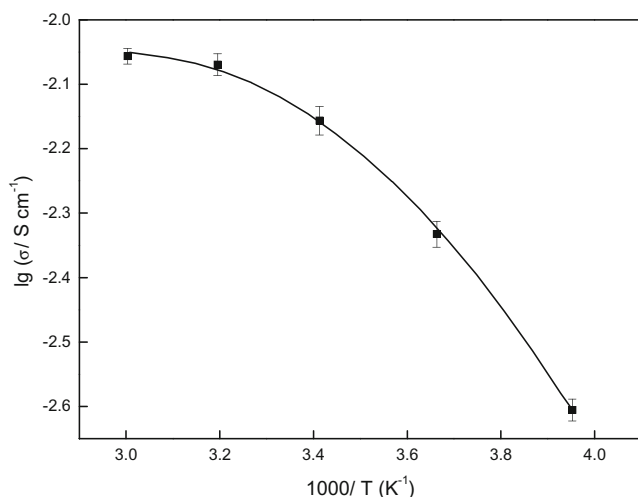


**Fig. 10** Arrhenius plot of ionic conductivity for the activated grafted PVDF fibrous membrane (DOG=111.8%)

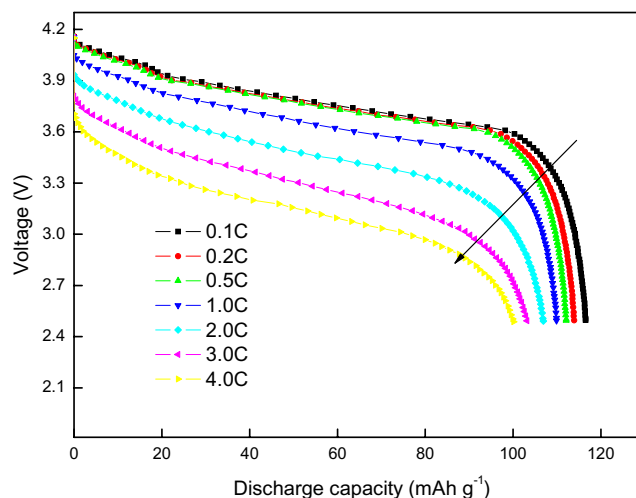


**Fig. 11** Discharge capacities of LiCoO<sub>2</sub>-MCMB coin cells containing the activated grafted PVDF fibrous membrane (DOG=111.8%) at different C rates. nominal capacity, 118 mAh g<sup>-1</sup>, 25 °C

mechanism of the membrane seemed to obey Vogel–Tammann–Fulcher (VTF) rule with the following equation:

$$\sigma = A/T^{-1/2} \exp[-E_a/k_b(T - T_0)] \quad (3)$$

where  $A$  was a constant proportional to the number of carrier ions,  $E_a$  was the pseudoactivation energy related to the polymer segmental motion,  $k_b$  was the Boltzmann constant, and  $T_0$  was a reference temperature at which the configurational entropy of the polymer became zero and was close to the glass transition temperature. In this work, the fitted value for the fibrous membrane ( $A=1.09 \text{ S cm}^{-1} \text{ K}^{1/2}$ ,  $E_a=1.14 \text{ eV}$ ) was obtained by plotting the VTF graph.

Figure 11 showed the discharge curves of the cell obtained at different current rates. This figure revealed that

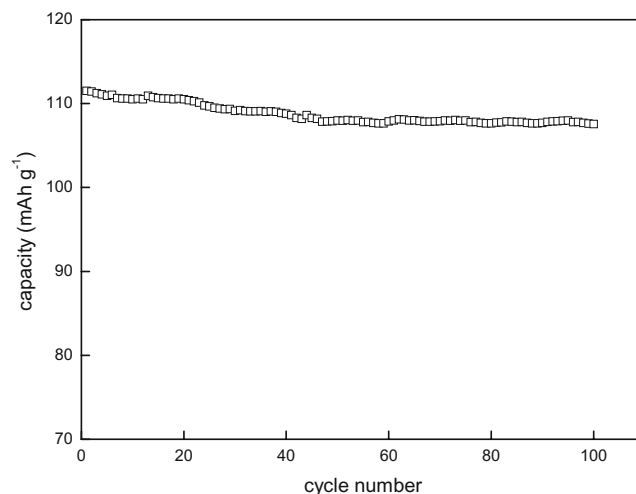


**Fig. 12** Cycle performance of LiCoO<sub>2</sub>-MCMB coin cells containing the activated nonwoven PVDF membrane (DOG=111.8%) at the 0.5C rate. 2.5–4.2 V, 25 °C

the cell at 0.1 C rate could achieve a good capacity of 116.5 mAh g<sup>-1</sup>. Furthermore, both the voltage and the capacity were found to be gradually decreased with increasing current rate. The large polarization resulted in reduction of the discharge mean voltage and capacity. It was also estimated that the tested cell still retained about 86% of discharge capacity at 4C rate, as compared to that at 0.1C rate. This excellent rate performance could be ascribed to the grafted PMMA layer which had good affinity for electrolyte and electrode.

Figure 12 showed the cycle performance of the grafted PVDF fibrous membrane applied in a lithium ion battery. The prototype cell was subjected to a cycle test under conditions with a cutoff voltage of 4.2 V for the upper limit and 2.5 V for the lower limit at a 0.5C rate. The prototype cell showed very stable charge/discharge properties, having little capacity fade under constant current and constant voltage conditions at the 0.5C rate.

## Conclusion

The combination of PMMA to the PVDF fibrous membrane was a novel approach to achieve high ionic conductive polymer electrolytes. The reason was that PMMA possessed good affinity for the liquid electrolyte and the gelled PMMA could substitute nonconductive PVDF to be in contact with the electrodes. A dual-phase PVDF-based fibrous membrane was prepared via preirradiation. Grafting PMMA onto the PVDF fibrous membrane made the fibers fatter. PMMA was incompatible with PVDF and showed obvious phase separation between them. The fibrous membranes could be activated by the liquid electrolyte. In this study, the highest ionic conductivity of the fibrous membrane in this study was  $7.9 \times 10^{-3}$  S cm<sup>-1</sup> at

room temperature, which was close to the liquid electrolyte. It showed an excellent rate performance. As compared to that at the 0.1C rate, the cell still retained about 86% of its discharge capacity at the 4C rate. The prototype cell using the PVDF fibrous-grafted membrane showed good cycle performance. Primary results showed that it was promising as a polymer electrolyte for a scaled-up lithium ion battery.

## References

1. Liu HK, Wang GX, Guo ZP (2006) *J Nanosci Nanotechnol* 6:1
2. Zhang SS (2007) *J Power Sources* 164:351
3. Stephan AM, Nahm KS (2006) *Polymer* 47:5952
4. Yuan LX, Piao JD, Cao YL (2005) *J Solid State Electrochem* 9:183
5. Kaneko M, Nakayama M, Wakihara M (2007) *J Solid State Electrochem* 11:1071
6. Zhao F, Wang MK, Qi L, Dong SJ (2004) *J Solid State Electrochem* 8:283
7. Wang XJ, Zhang HP, Kang JJ (2006) *J Solid State Electrochem* 11:21
8. Kim JR, Choi SW, Jo SM (2004) *Electrochim Acta* 50:69
9. Cho TH, Sakai T, Tanase S (2007) *Electrochem Solid St* 10:A159
10. Matsuda Y, Takemitsu T, Tanigawa T, Fukushima T (2001) *J Power Sources* 97–98:589
11. Choi SW, Kim JR, Ahn YR (2007) *Chem Mater* 19:104
12. Kim JR, Choi SW, Jo SM (2005) *J Electrochem Soc* 152:A295
13. Nicotera I, Coppola L, Oliviero C, Castriota M (2006) *Solid State Ionics* 177:581
14. Mahendran O, Rajendran S (2003) *Ionics* 9:282
15. Nicotera I, Coppola L, Oliviero C, Ranieri GA (2005) *Ionics* 11:87
16. Missan HPS, Sekon SS (2005) *J Mater Sci* 40:3771
17. Bhattacharya A, Misra BN (2004) *Prog Polym Sci* 29:767
18. Takacs E, Mirzadeh H, Wojnarovits L (2007) *Nucl Instrum Methods B* 265:217
19. Brack HP, Buhner HG, Bonorand L, Scherer GG (2000) *J Mater Chem* 10:1795
20. Li WL, Xu LX, Luo D, Yang MJ (2007) *Eur Polym J* 4:522
21. Agnihotry SA, Nidhi, Pradeep, Sekhon SS (2000) *Solid State Ionics* 136:573